ELSEVIER

Journal of Crystal Growth 196 (1999) 511–523

JOURNAL OF CRYSTAL GROWTH

X-ray diffraction studies of protein crystal disorder

I. Dobrianov[a], C. Caylor[a], S.G. Lemay[a], K.D. Finkelstein[b], R.E. Thorne[a,*]

[a] *Laboratory of Atomic and Solid State Physics, Cornell University, Ithaca, NY 14853, USA*
[b] *Cornell High-Energy Synchrotron Source (CHESS), Ithaca, NY 14853, USA*

Abstract

Protein crystals contain many kinds of disorder, but only a small fraction of these are likely to be important in limiting the diffraction properties of interest to crystallographers. X-ray topography, high-angular-resolution reciprocal space measurements, and standard crystallographic data collection have been used to probe three factors that may produce diffraction-limiting disorder: (1) solution variations during crystal growth, (2) macromolecular impurities, and (3) post-growth crystal treatments. Variations in solution conditions that occur in widely used growth methods may lead to variations in equilibrium protein conformation and crystal packing as a crystal grows, and these may introduce appreciable disorder for sensitive proteins. Tetragonal lysozyme crystals subjected to abrupt changes in temperature, pH, or salt concentration during growth show increased disorder, consistent with this mechanism. Macromolecular impurities can have profound effects on protein crystal quality. A combination of diffraction measurements provides insight into the mechanisms by which particular impurities create disorder, and this insight leads to a simple approach for reducing this disorder. Substantial degradation of diffraction properties due to conformation and lattice constant changes can occur during post-growth crystal treatments such as heavy-atom compound and drug binding. Measurements of the time evolution of crystal disorder during controlled crystal dehydration – a simple model for such treatments – suggest that structural metastability conferred by the constraints of the crystal lattice plays an important role in determining the extent to which the diffraction properties degrade.

PACS: 61.72; 81.10; 87.15

Keywords: Protein crystal growth; Crystal disorder, Protein crystallography; X-ray topography

1. Introduction

A detailed understanding of the function of proteins and other biological macromolecules requires knowledge of their three-dimensional structure. The accuracy of structures determined by X-ray crystallography is limited by disorder present in crystallized proteins. Consequently, the most important goals of fundamental studies of protein crystal growth are to identify and reduce this disorder [1–7].

The work described here is motivated by a number of basic questions, including: (1) What kinds of

* Corresponding author. Tel.: + 1 607 255 6487; fax: + 1 607 255 6428; e-mail: ret6@cornell.edu.

0022-0248/99/$ – see front matter
PII: S0022-0248(98)00833-1

disorder do protein crystals exhibit? (2) How do particular kinds of disorder affect the X-ray diffraction properties? (3) What properties of the molecules and their interactions are most relevant in producing disorder? (4) How does disorder arise during and after growth? and (5) How much of the disorder can be eliminated by proper choice of growth method?

Section 2 begins with a review of X-ray diffraction measures of protein crystal quality, and Section 3 speculates on the kinds of disorder that contribute in limiting each of these measures. Sections 4 and 5 give an overview of X-ray diffraction studies that are investigating three factors that may produce diffraction-limiting disorder: solution variations during crystal growth, macromolecular impurities, and post-growth crystal treatments. Section 4 describes the experimental methods. Section 5 discusses how each of these factors may create disorder and presents the experimental results. More detailed discussion of these studies will be given elsewhere [8–10].

2. X-ray diffraction measures of protein crystal disorder

Three primary measures are used by macromolecular crystallographers to characterize protein crystal diffraction quality: the diffraction resolution, the B or temperature factor, and the mosaicity [6,11]. What do these parameters reveal about crystal disorder, and how are they related to each other and to specific kinds of disorder?

2.1. Diffraction resolution

The maximum scattering angle $(2\theta)_{\max}$ at which diffraction peak intensities can be reliably measured determines the diffraction resolution $d_{\min} = \lambda/2 \sin[(2\theta)_{\max}/2]$, and limits the spatial resolution of the electron density map that can be derived from the diffraction data. The diffraction resolution depends upon several factors [6,11], including the overall intensity scale of the diffraction pattern, how rapidly the diffracted intensity falls off with scattering angle, the background diffuse scattered intensity, and the instrumental noise of the detector system. These depend in turn upon crystal properties like the crystal volume, unit cell size, B factor, and mosaicity; on incident X-ray beam characteristics including the flux and source size/divergence; and on data collection parameters such as the oscillation step size and integration time. Because so many factors are involved, the diffraction resolution provides a poorly defined measure of crystal disorder, even though it is the most important measure for crystallographers.

2.2. B factor

The B or "temperature" factor is used to characterize the fall-off of diffracted intensity I with scattering angle, according to $I \propto \exp[-2B \sin^2 \theta/\lambda^2]$. Unlike the diffraction resolution, the overall B factor obtained from a Wilson analysis is determined primarily by the properties of the crystal, and can be more reliably used to compare crystals measured in different laboratories. Typical protein crystal B factors range from 5–100 Å^2 compared with <1 Å^2 for small molecule crystals, and correspond (in a simple Debye–Waller analysis) to rms atomic displacements on the order of 1% of the molecular diameter. Although random thermal motion usually limits the B values of small-molecule crystals, static or quasi-static disorder often dominates in protein crystals (particularly when data are collected using frozen crystals).

The B factor is essentially a measure of short-range lattice order [12]. Crudely, it measures how far the positions of each atom or molecule in a lattice deviates from the *locally defined* average lattice orientation and spacing. It is sensitive to lattice disorder on the scale of several unit cells, and not to long-range disorder produced by, e.g., grain boundaries or sectoriality. For example, the B factor is largely unaffected when a metal crystal is ground into a powder with 1000 Å grains [12,13]; the long-range lattice order is destroyed, but the local order within each grain is preserved. Defects such as vacancies, interstitials, impurities, dislocations, grain boundaries, twins, cracks, and inclusions produce appreciable atomic and molecular displacements from the locally defined lattice grid only in their immediate vicinity; for point defects like vacancies, nearly all of their effect on B is due to

displacements of their first-nearest-neighbor molecules [12,14,39]. Consequently, the B factor is insensitive to most kinds of lattice defects except when they are present at extremely high concentrations. On the other hand, subtle but pervasive kinds of disorder such as small molecular conformation variations and small molecular displacements and rotations from site to site within the lattice can have large effects on B.

2.3. Mosaicity

The mosaic width of a reflection is defined as the range of angles $\Delta\theta$ over which a crystal will continue to diffract strongly at a fixed, *well-defined* 2θ when the crystal is rotated about an axis θ perpendicular to the plane defined by the incident and diffracted X-ray beams. The measured mosaic width $\Delta\theta$ is a convolution of the intrinsic width η of the crystal and an instrumental resolution $(\Delta\theta)_{IR}$. This width differs from the mosaicity parameter generated by standard analysis programs like Scalepack; the mosaicity parameter includes the effects of X-ray beam crossfire and energy spread and uses a different definition of peak width[1], and thus can be much larger than $\Delta\theta$ and η when these are small. Protein crystals that are well faceted and not twinned usually have mosaic full-width at half-maximums (FWHMs) – 0.02° or less [8,20–23,46–50] – that are very small even by small-molecule crystal standards, but these generally become larger – 0.1° or more – when crystals are frozen for data collection. Even when crystals have narrow mosaic widths, crystallographers usually do not match the incident X-ray beam divergence to the angular acceptance of the crystal. Consequently, the as-grown mosaic widths seldom dominate in data collection.

The mosaic width is a measure of lattice orientational order, and is sensitive to disorder on a broad range of length scales. Thus, it is useful to distinguish between "macroscopic" mosaicity, in which lattice orientation variations occur on a length scale smaller than but comparable to the crystal size, and "microscopic" mosaicity, in which orientation variations occur on a scale much smaller than the crystal size. Macroscopic mosaicity may arise due to twinning, grain boundaries, sectoriality, and cracks, and a single macroscopic defect can be sufficient to produce a large mosaic width. Macroscopic mosaicity may also result from elastic crystal bending due to the forces exerted by mounting for X-ray data collection; in fact, X-ray topography measurements suggest that this can be the largest contribution to the measured mosaic widths, particularly for flat or needle-like crystals. Microscopic mosaicity may arise from dislocations, inclusions, and perhaps also random accumulation of molecular disorder. Mosaicity of any type can affect the diffraction resolution by affecting the overall peak-to-background ratio. Only microscopic mosaicity can in principle affect the fall-off of Bragg peak intensity with scattering angle (the B factor), by disrupting the short-range lattice order within an appreciable fraction of the crystal volume through lattice bending. In fact, the measured mosaic widths are orders of magnitude too small to directly account for the observed B factors, so that microscopic mosaicity may at best be a symptom of the B-factor-limiting disorder, and may *correlate* with B.

2.4. Which types of disorder limit the diffraction properties of protein crystals?

Protein crystal disorder has been characterized using a wide variety of techniques [15–18,40–45], and the defects that have been observed or inferred–twins, stacking faults, sectorial discontinuities, growth bands and ghosts, inclusions, dislocations, vacancies, interstitials, and impurity macromolecules – parallel those observed in small-molecule crystals. The types of disorder that dominate the mosaicity – twins, grain boundaries, sectorial misorientation, cracks, and dislocations – are fairly obvious. But which types limit the protein crystal B factors?

Total defect densities (point defects, inclusions, and dislocations) observed by AFM [19,42–45] in several proteins are generally less than 10^5–10^6 cm^{-2}; dislocation densities can be as high as 10^6 cm^{-2}, although

[1] The mosaicity parameter in Scalepack is obtained by fitting the peak intensity profile with $I \propto (1 + \cos[\alpha(\theta - \theta_{peak})])$, and corresponds to the width in θ that produces a variation of the argument of the cosine from $-\pi$ to $+\pi$. This width is roughly twice the FWHM of a gaussian or lorentzian-shaped peak.

crystals of many proteins show no evidence of dislocations. As discussed in Ref. [8], these defect densities are roughly six orders of magnitude smaller than those needed in metal and small-molecule crystals to produce measurable effects on B factors. Even when their much larger lattice constants are accounted for, the observed defect densities in protein crystals appear to be orders of magnitude too small to account for the observed B values. This suggests that (1) the most common small-molecule types of crystal disorder and thus the most common disorder-producing mechanisms may be unimportant in limiting protein crystal B values; (2) the important disorder may not be directly visible in AFM; and (3) the dominant disorder is likely due to conformation variations, chemical microheterogeneity, small molecular displacements and rotations from site to site within the crystal, and perhaps also to macromolecular impurities when present at very large concentrations.

3. Experimental characterization methods

The experimental studies of protein crystal disorder to be described in the next section employed three different X-ray characterization techniques: X-ray topography [19,20,46–48], high angular and wave-vector resolution reciprocal space scans [21–23,49,50] , and standard crystallographic data collection.

X-ray topography measurements are performed by illuminating a crystal using a highly parallel monochromatic X-ray beam and recording the diffraction pattern using high-resolution film placed very close to the crystal [19,20,46–48]. Under these illumination conditions, the diffraction from different points in the crystal is spatially resolved at the film, and the diffraction spots provide images of the crystal. Crudely; image contrast results from variations in the diffracted intensity due to variations in lattice orientation and spacing associated with crystal defects and strains. X-ray topography probes *bulk* crystal perfection; the "topography" in this case is of the diffracting planes within the crystal [19]. It has been widely used to characterize small-molecule crystals, revealing dislocations, twins, grain boundaries, growth bands and ghosts, inclusions, and other disorder, and has recently been applied to protein crystals [20,46–48].

Image sensitivity to lattice orientation variations is determined by the angular divergence $\Delta\phi$ of the beam incident on the sample (determined by the X-ray source size and the source-to-sample distance). The minimum spatial resolution Δx of the image is determined by the angular divergence $\Delta\phi$ and the film-to-sample distance d according to $\Delta x \approx d\,\Delta\phi$. It is also limited by the film grain size and, if the film is not perpendicular to the reflection, by the emulsion thickness. Most of the data described here have been taken on CHESS station B-2 using a double-bounce Si(1 1 1) monochromator, which provides a maximum angular sensitivity of 0.002° ($7''$). The 3 cm sample-to-film distance gives a minimum image resolution of 2 μm. Images were recorded using Kodak Industrex SR film. To date, topographs of more than 300 protein crystals have been recorded.

Fig. 1 shows four topographs illustrating applications of this technique. Fig. 1a and Fig. 1b show topographs of a lysozyme crystal and a canavalin crystal, respectively. The lysozyme crystal shows little contrast (aside from that associated with sectoriality) and no sharp contrast that would indicate the presence of bulk defects. The canavalin crystal (provided by A. Malkin) shows extensive contrast, including sharp lines indicating the presence of dislocations arranged in a pattern very similar to that observed in many inorganic crystals [24]. AFM measurements [18,42–45] have shown that lysozyme crystals grown under similar conditions exhibit very few dislocations, whereas canavalin crystals show high dislocation densities, consistent with the topographs. Fig. 1c shows a topograph of a needle-like catalase crystal (provided by A. Malkin), only a small portion of which is visible due to lattice bending. AFM studies on these crystals [18,42–45] have observed incorporation of microcrystals having sizes of microns to tens of microns. Evidence for an incorporated microcrystal is visible in the topograph. Fig. 1d shows a topograph of a tetragonal lysozyme crystal that has been soaked in cryoprotectant and then flash-frozen. The contrast in this case is difficult to interpret, but the crystal has developed microcracks and a broad mosaic width.

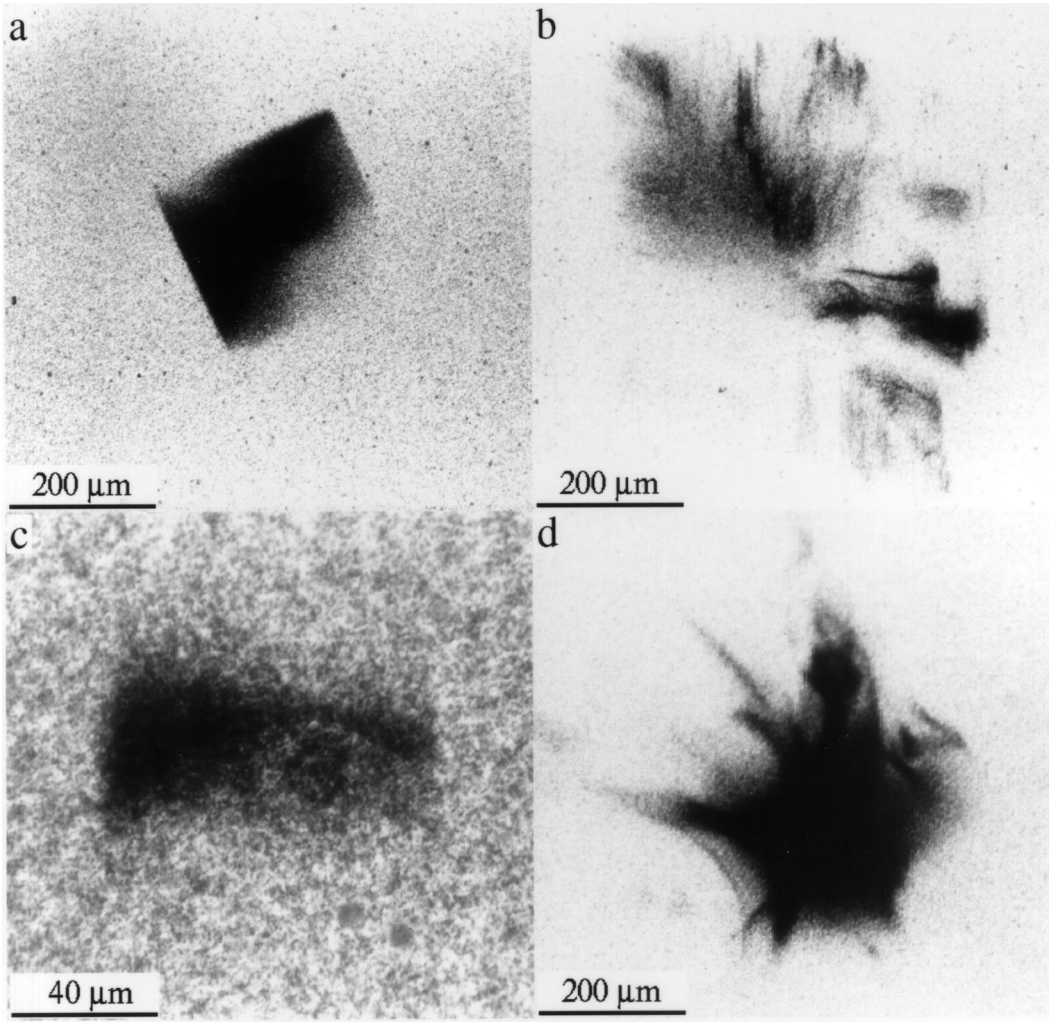

Fig. 1. X-ray topographs of crystals of (a) tetragonal lysozyme, (b) canavalin, and (c) catalase. The crystal in (d) is a tetragonal lysozyme crystal that has been flash-frozen using a standard liquid nitrogen cryocooler.

High angular and wave-vector resolution reciprocal space scans of selected Bragg reflections were performed on CHESS station C-2 using a Si(1 1 1) double-bounce monochromator, a Si(1 1 1) analyzer crystal, and a six-circle diffractometer. Mosaic scans [21–23,49,50] – measuring the distribution of lattice orientations in the crystal – were performed by rocking the crystal about the θ axis while recording the diffracted intensity at fixed 2θ using the analyzer crystal and a scintillation detector. θ–2θ scans – measuring the distribution of lattice spacings within the crystal – were performed by scanning θ and 2θ together; this corresponds to a radial scan in reciprocal space through the Bragg peak.

Standard crystallographic data collection was performed on CHESS stations B-2 and C-2, using image plates to record the diffraction patterns. The programs Denzo and Scalepack were used to index and merge the data and to calculate lattice constants. Subroutines from the CCP4 package were used to generate Wilson plots and to estimate B factors.

4. Results and discussion

4.1. Effects of solution variations during growth

One significant difference between proteins and small molecules is that proteins have many more internal degrees of freedom. Proteins show extensive conformational flexibility, particularly of regions near their surface that can be important in crystal packing, and this can lead to significant "intrinsic" crystal disorder that cannot be eliminated by proper choice of growth method. Proteins are also much more sensitive to their solution environment. Changes in pH, salt concentration, temperature, and other parameters can induce significant changes in protein conformation and hydration. As a result, protein crystals show extensive polymorphism, and lattice constants for a given polymorph can show enormous variations (in some cases as large as 10%) when growth conditions are changed.

The strong sensitivity of proteins to their solution environment suggests a mechanism by which the molecular-scale disorder affecting B factors might be produced. In the growth methods used in the overwhelming majority of crystallizations [1,2], solution conditions can vary substantially during the growth of an individual crystal. For example, in vapor diffusion growth, the concentrations of all solutes within the drop can vary by a factor of two or more as the drop equilibrates with the well, and there can be significant changes in pH [25]. Solution conditions can also vary due to protein depletion and solute rejection by growing crystals [26,27]. Because of these solution variations, the equilibrium protein conformation, crystal solvent content, and crystal lattice constant should vary during growth of a given crystal. As growth proceeds, interior regions may attempt to relax towards the evolving equilibrium, and molecular-scale disorder may result if there are energy barriers that lead to metastability in this relaxation or if there is degeneracy in the possible molecular configurations. Interior relaxation may produce a change in lattice volume, and stresses resulting from interior expansion or contraction may introduce further disorder. Solution variations during growth could also introduce disorder by more conventional mechanisms [7,27,28,51–53], for example by causing changes in growth kinetics that favor defect-forming instabilities like step bunching or that produce nonuniform impurity incorporation.

To investigate the effects of solution variations during growth on the perfection of tetragonal hen egg white lysozyme (HEWL) crystals [8], crystals were grown under uniform and nonuniform conditions using Seikagaku lysozyme ($6\times$ recrystallized) in acetate buffer at pH near 4.5 using NaCl as the precipitant. Nearly uniform growth conditions were achieved by performing batch growth in large hanging drops, and by removing crystals from drops for X-ray measurements before protein depletion was appreciable. To obtain time-varying conditions, crystals were grown by this batch method in one solution and then transferred to a second drop that provided different solution conditions (pH, salt concentration, protein concentration, and temperature) for subsequent growth. Tetragonal lysozyme is not particularly well suited to this kind of study, since its lattice constants show limited variation over a broad range of conditions. To simulate the behavior of more sensitive proteins, somewhat larger changes in conditions than is typical of lysozyme growth were explored.

Fig. 2 shows X-ray topographs of four lysozyme crystals. Fig. 2a shows a topograph of a crystal grown under nearly uniform conditions. There is no evidence of disorder, and the diffracted intensity varies smoothly over the image in a manner suggestive of a gradual bending of the lattice. Fig. 2b and Fig. 2c show topographs of crystals subjected to abrupt changes in pH and salt concentration, respectively, midway during their growth; in both cases the protein concentration of the final solution was adjusted to minimize the change in growth rate. These crystals show a significant difference in diffracted intensity between the pre- and post-change growth regions. Fig. 2d shows a crystal subjected to a larger change in salt concentration that, due to incomplete mixing, produced protein-rich droplets that dissipated within 20 min after the change. The topograph shows dislocations radiating in characteristic directions from the pre-change crystal boundary and inclusions near the boundary.

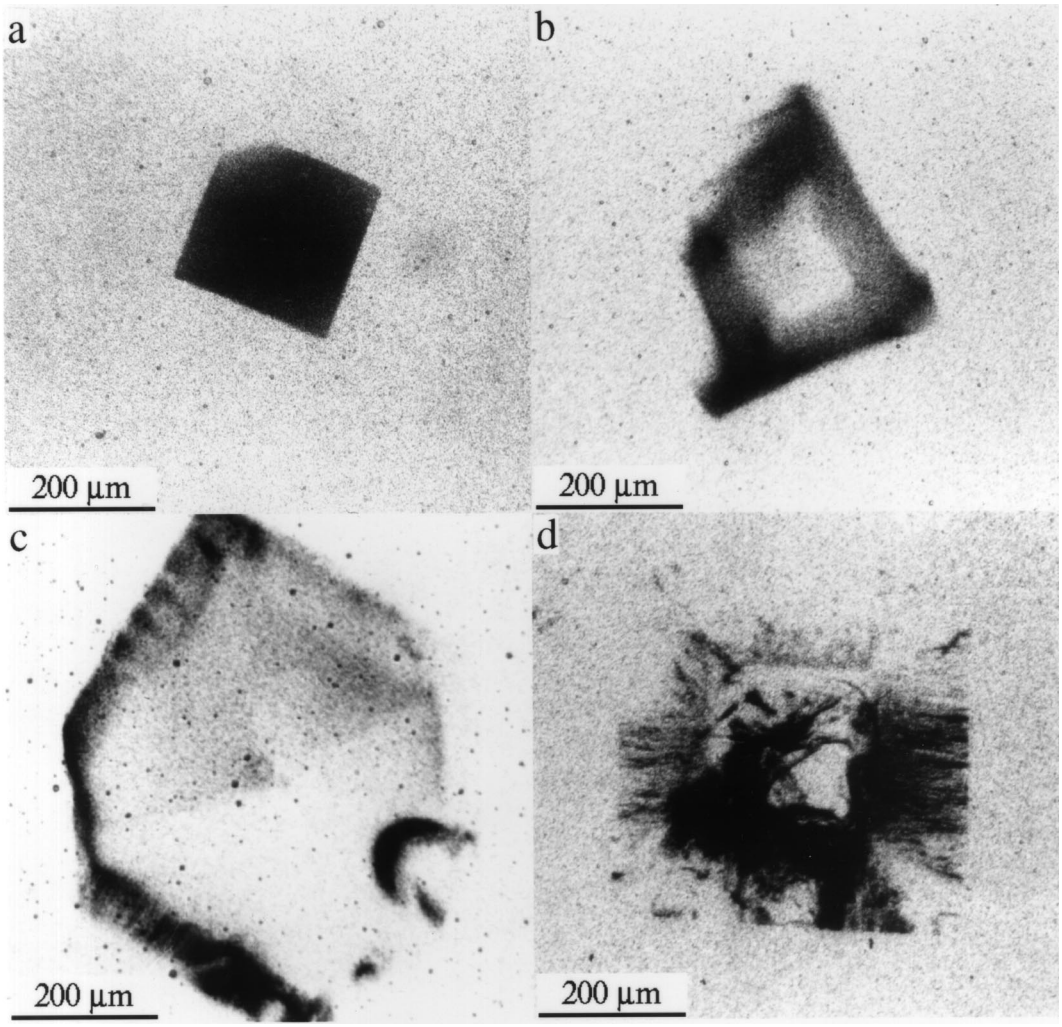

Fig. 2. X-ray topographs of four tetragonal lysozyme crystals grown at $T = 21°C$ in acetate buffer with NaCl as the precipitant. (a) A crystal grown under nearly uniform conditions. (b) A crystal subjected to an abrupt change in solution pH from 5 to 4 midway during growth. (c) A crystal subjected to an abrupt change in salt concentration from 0.5 to 1.0 M midway during growth. (d) A crystal subjected to a 0.4 to 1.2 M change in salt concentration that produced transient precipitate or protein-rich droplets. In (b)–(d), the protein concentration was adjusted to maintain an approximately constant growth rate before and after the change in solution conditions.

To determine the origin of the contrast seen in the topographs of Fig. 2, high-resolution mosaic and θ–2θ scans were acquired. Mosaic FWHM values for uniform growth crystals are only a few thousandths of a degree, comparable to those reported for microgravity-grown lysozyme crystals [22,49,50], whereas peaks with significantly larger FWHM values and broader tails are observed for crystals subjected to a changes in pH or salt concentration. θ–2θ scan widths are essentially resolution-limited for both uniform and nonuniform growth crystals, indicating that the crystals are not on average appreciably strained. Topographs acquired at successive angles in the mosaic curve of a given reflection show that the mosaic width of the pre-change growth region is comparable to that of

uniform growth crystals, whereas the width of the post-change growth region is larger. Analysis of diffraction patterns acquired for representative crystals do not show large effects of solution changes on crystal *B* factors, but this is not surprising given the robustness of lysozyme.

The additional disorder observed in the post-change growth region could arise in several ways. First, the change in solution conditions could produce changes in growth kinetics that favor defect-forming instabilities or nonuniform impurity incorporation [7,27,28,51–53]. However, abrupt changes in protein concentration that change the growth rate by a factor of three (while leaving pH and salt concentration fixed) produce no visible contrast in topographs. Second, the shock of the change in solution conditions could create disorder in the pre-change crystal core that then propagates outward into the post-change growth region. However, the core shows no evidence of increased disorder. Third, as discussed above, relaxation of the pre-change growth region after the change may induce disorder in the post-change growth region. From previous data [29], the changes in salt concentration investigated should have produced changes in lattice constant of roughly 0.2%, which would produce a change in the linear dimension of the pre-change growth region of roughly 0.5 μm. Changes of this magnitude make plausible the notion that lattice relaxation could be the source of the observed disorder.

These experiments provide evidence that solution variations during growth, including those typical of vapor diffusion growth, macro-seeding, and other widely used techniques, can create disorder in protein crystals. Additional experiments on more typical and sensitive proteins are required to establish if these variations can have appreciable effects on crystal *B* factors.

4.2. Effects of macromolecular impurities

In practical crystal growth as practiced by macromolecular crystallographers, growth solution purity is one of the most important factors affecting crystal and diffraction quality [1,2]. Protein crystal growth solutions contain a wide variety of macromolecular impurities, usually at total concentrations of at least several molecular percent. Even "high-purity" commercial lysozyme contains at least one percent macromolecular impurities [30–32,54,55]. These impurities can have profound effects on crystal growth, producing reduced or increased solubility, suppressed or enhanced nucleation, changes in growth habit and morphology, and causing formation of twins and polycrystalline or amorphous aggregates [30–34,54–61].

What are the mechanisms by which impurities affect protein crystal quality? First, impurities may incorporate either substitutionally or interstitially into the lattice of a growing crystal. Impurities produce changes in lattice constant, and nonuniform incorporation due to nonuniform growth rates or to different incorporation rates in different growth sectors [7] leads to lattice constant variations. The resulting strains can cause cracks, dislocations and other defects that increase the crystal mosaic width. Impurities can also degrade *B* factors by causing displacements of nearby molecules, but this effect is likely small except at very large incorporated densities [8,9]. Bulk lattice incorporation is most likely for genetic or chemical variants that are structurally similar to the host macromolecule; structurally dissimilar impurities are generally preferentially rejected during growth.

Second, impurities may reduce crystal quality by affecting ordering in the initial stages of growth. As discussed by Vekilov et al. [27], impurities are more likely to be incorporated in crystal cores. Aggregates containing impurities may form highly imperfect nuclei, leading to formation of grain boundaries and a high density of dislocations that propagate outward into subsequent growth regions, broadening the crystal mosaic width but having little effect on *B* factors. This mechanism should be much less sensitive to similarity between the impurity and the host macromolecule.

Third, impurities may affect growth kinetics in ways that favor defect-forming instabilities such as step-bunching [7,28,51–53], possibly broadening crystal mosaic widths but again having little effect on *B* factors. This mechanism is likely important in growth at low supersaturations and in cessation of growth.

The effects of impurities on tetragonal hen egg white lysozyme crystals are being investigated [9]

using the X-ray diffraction techniques described in Section 3. Following earlier work [30,32–34, 55–61], two different impurities are being used: turkey egg white lysozyme (TEWL), which is structurally extremely similar to HEWL and thus is expected to incorporate within the bulk lattice; and ovotransferrin, a structurally dissimilar impurity.

Fig. 3a and Fig. 3b show X-ray topographs of crystals grown from solutions containing 20% TEWL and 5% ovotransferrin, respectively. For TEWL concentrations of 20% and larger, topographs often show evidence of cracks and dislocations, but well-faceted single crystals are frequently obtained even at concentrations above 20%. For ovotransferrin concentrations of 5%, topographs often show cracks and dislocations, but some crystals show no obvious disorder. Unlike TEWL, ovotransferrin has large effects on crystal nucleation and morphology: at concentrations above 5%, only complex polycrystals form, and nucleation is greatly suppressed at concentrations above 20%.

Mosaic scans on crystals grown in 5–20% TEWL and 2–5% ovotransferrin solutions yield relatively broad peak FWHM values of 0.01–0.03°, and usually show a complex, multi-peak structure with very broad wings, consistent with the observed crystal cracks. θ–2θ scans yield similar, essentially resolution-limited peak widths for pure and 5% ovotransferrin crystals, whereas the peak width of 20% TEWL crystals is substantially broadened, indicating the presence of a distribution of lattice constants. Neither impurity at any growth solution concentration has any measurable effect on crystal B values [36]. These results suggest that TEWL incorporates at high concentrations in the bulk of the crystal lattice, consistent with results for HEWL incorporation in TEWL [34], whereas ovotransferrin does not, consistent with recent chemical analysis [35].

If ovotransferrin does not incorporate appreciably in the bulk, then from the above discussion its primary effects may be in creating disorder in the early stages of growth. Consequently, it may then be possible to grow high-quality crystals from very impure solutions simply by providing an ordered nucleus. To test this idea, seed crystals have been grown from "pure" commercial lysozyme, and then placed in solutions containing 20% ovotransferrin.

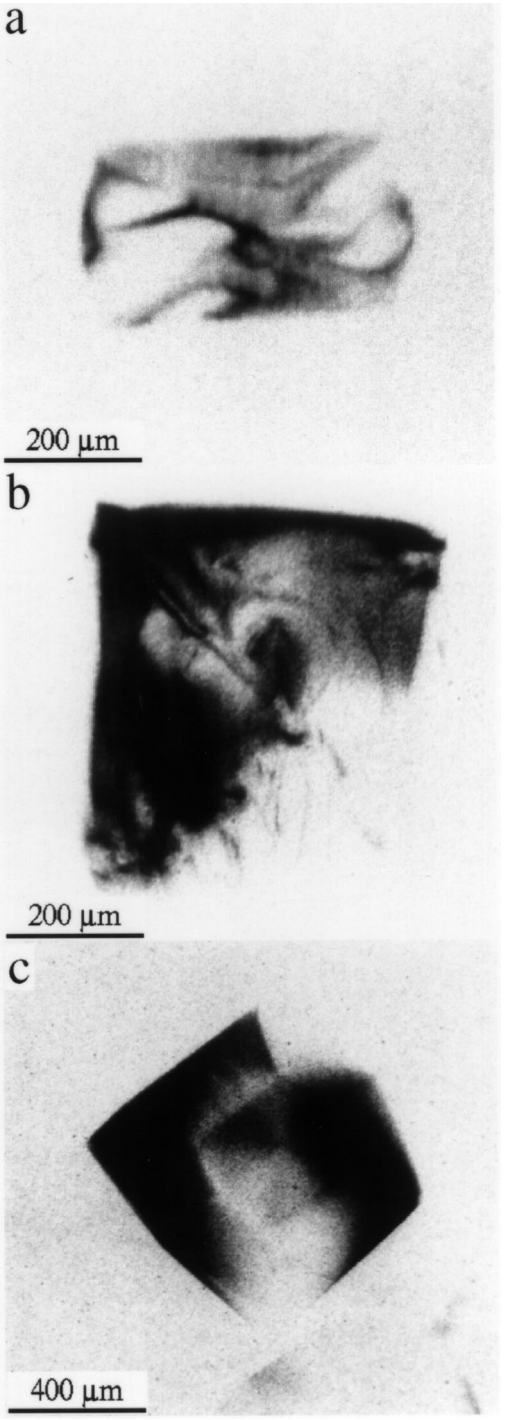

Fig. 3. X-ray topographs of tetragonal hen egg white lysozyme crystals grown from solutions containing (a) 20% turkey egg white lysozyme and (b) 5% ovotransferrin.

Spontaneous nucleation in such contaminated solutions results only in polycrystalline "balls", but when a pure seed is introduced, a well-faceted single crystal results. Fig. 3c shows an X-ray topograph of such a seed-grown crystal. Aside from contrast at the boundary between the seed and subsequent growth, there is no evidence of disorder. Mosaic widths, *B* factors, and diffraction resolutions of these seeded crystals are comparable to those grown from pure solutions. These results suggest a general tactic for obtaining crystals from heavily contaminated solutions when small amounts of purified protein–sufficient to make seeds–can be obtained.

4.3. Effects of post-growth crystal treatments

The disorder that limits the diffraction resolution of protein crystals is often caused by treatments–including heavy-atom compound binding, binding of substrate or drug molecules, and cryoprotectant soaks–performed *after* the crystal is grown [1,2,6,11]. These post-growth treatments share several features: they involve diffusive transport of molecules into the crystal; they often cause changes in lattice constant, lattice symmetry, and molecular conformation that lead to lattice strains, crystal cracking, and mosaic width broadening; and they usually degrade (but occasionally improve) crystal *B* factors and diffraction resolutions. A simple post-growth treatment that shares these general features is crystal dehydration. Water diffusion out of tetragonal lysozyme crystals causes a decrease in lattice constant, and larger dehydrations cause a change in molecular conformation and a substantial degradation of the diffraction resolution [29,38].

The effects of controlled dehydration on the perfection of tetragonal hen egg white lysozyme crystals are being investigated [10] using the techniques described in Section 3. Crystals are mounted in X-ray capillaries together with a plug of saturated salt solution. Using different salts, equilibrium relative humidities (r.h.) between 97 and 75% are obtained [29,37,38,62]. For comparison, typical NaCl concentrations used in lysozyme crystal growth experiments yield r.h. values between 95 and 99%.

Fig. 4 shows topographs of two lysozyme crystals dehydrated to 85% relative humidity. For relative humidities greater than 90%, the unit cell volume changes by less than 1%, and the topographs are as featureless as those of nondehydrated crystals. *B* factors and diffraction resolutions for these crystals are also indistinguishable from those of nondehydrated crystals. For relative humidities less than 90%, the unit cell changes are much larger and the topographs show extensive contrast that is highly suggestive of a crystal drying out. Some

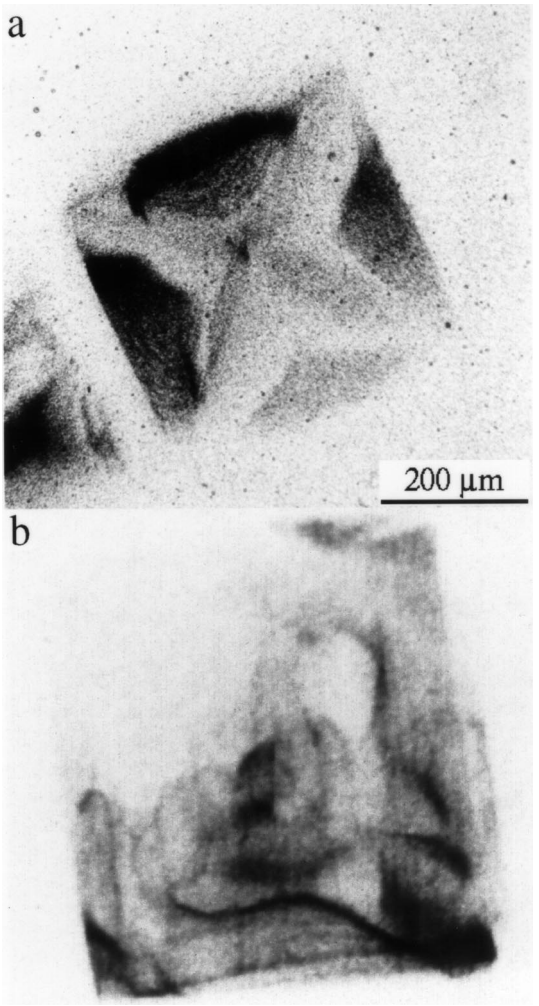

Fig. 4. X-ray topographs of two tetragonal lysozyme crystals subjected to dehydration to 85% relative humidity by equilibration with vapor over an aqueous salt solution.

crystals show obvious cracks and the most heavily dehydrated crystals can show web-like patterns of dislocations and microcracks. Diffraction patterns of crystals dehydrated to 83% r.h. and lower are severely degraded, and only a few reflections near the beam stop corresponding to $d > 6$ Å are typically observed.

To understand how this disorder develops, topographs and diffraction patterns have been recorded in situ as dehydration progresses. Fig. 5 shows a series of topographs acquired during dehydration of a lysozyme crystal to 81% r.h. The evolution of contrast in the topographs is largely complete 2–3 h after the start of dehydration, and lattice constants deduced from the diffraction pattern reach steady-state values in roughly the same time. However, the diffraction resolution and B factor remain largely unchanged for the first 24 h, and have degraded dramatically only after 31 h. This implies that the disorder that degrades the B factor and diffraction resolution develops long after the water content of the crystal has decreased to near the equilibrium value appropriate to the relative humidity. Measurements on similar crystals under similar dehydration conditions show that while the times for the topographs and lattice constants to evolve are quite reproducible, the time for appreciable degradation of the diffraction pattern varies significantly, from as little as 1 h to as much as several days.

These results suggest that after water removal the lysozyme molecules remain in an ordered metastable configuration, stabilized by crystal contacts, before undergoing conformational changes and/or displacements and rotations in the unit cell. Whatever changes occur are not reproducible from unit cell to unit cell, and this causes degradation of the diffraction pattern. The origin of the two order-of-magnitude variation in time scale for the degradation of the diffraction is unclear, but the presence or

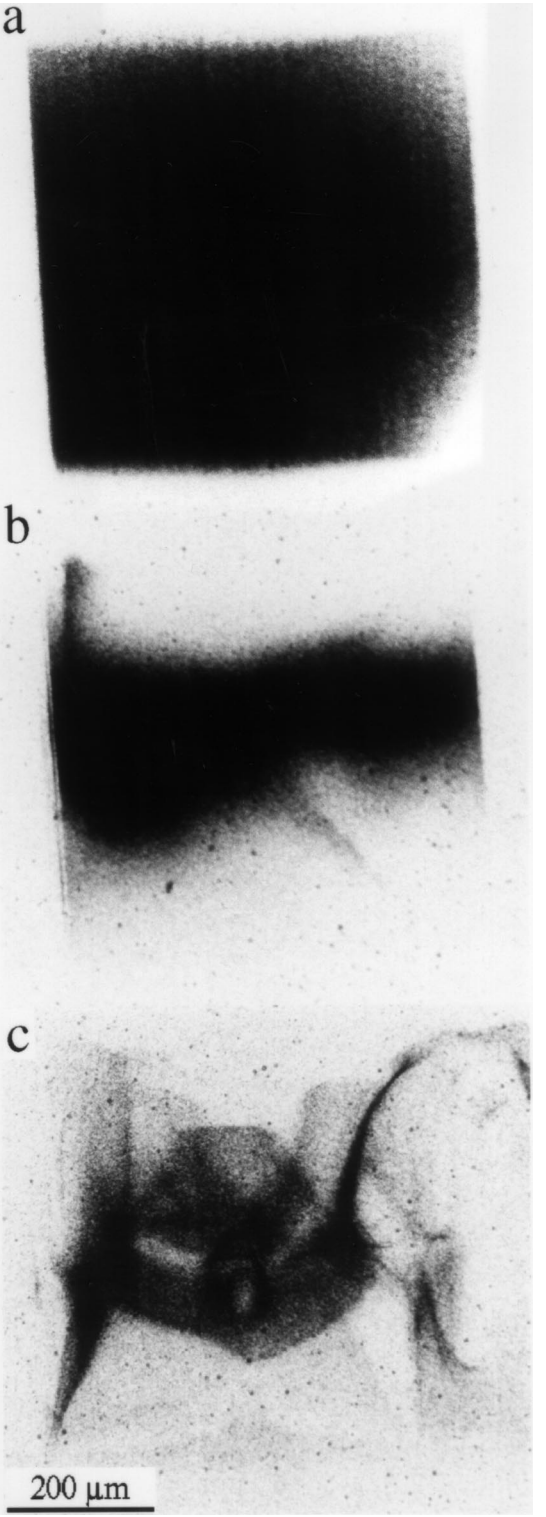

Fig. 5. Time series of topographs during dehydration to 81% relative humidity for a tetragonal lysozyme crystal. The topographs were acquired at (a) $t = 0$, (b) $t = 60$ min, and (c) $t = 23$ h after the start of dehydration. Because the lattice constants decrease and the diffraction pattern changes, the images were acquired from the same region of the diffraction pattern, but using different reflections.

absence of dislocations and cracks that may facilitate molecular relaxation may play a role. An understanding of the factors responsible for the variable decay of the diffraction may help in improving the success of more general post-growth treatments: when the conformation or lattice change associated with a given treatment cannot be achieved without introducing substantial equilibrium disorder, then the treatment's success may depend upon maintaining the lattice in a metastable configuration.

5. Conclusion

An understanding of the relation between disorder and diffraction can provide an important guide in attempts to prepare high-quality crystals of biological macromolecules. The experiments described here have focussed on three factors–solution variations during growth, macromolecular impurities, and post-growth crystal treatments–and have provided insight as to the disorder each produces and the effects each has on the diffraction properties. These experiments demonstrate the power of using X-ray topography in concert with other diffraction techniques. By coordinating use of these techniques with molecular-scale real-space probes like atomic force microscopy and electron microscopy, a detailed understanding of protein crystal disorder may soon be possible.

Acknowledgements

We wish to thank B. Batterman, R. Blessing, J. Brock, A. Chernov, R. Collela, G. DeTitta, S. Ealick, R. Maimon, A. Malkin, Z. Otwinowski, E. Snell, B. Thomas, P. G. Vekilov, and W. Webb for fruitful discussions and C. Kimmer for technical assistance. This work was supported by NASA (NAG8-1357).

References

[1] A. McPherson, Preparation and Analysis of Protein Crystals, Krieger, Malabar, 1982.
[2] A. Ducruix, R. Giege (Eds.), Crystallization of Nucleic Acids and Proteins, IRL, Oxford, 1992.
[3] A. McPherson, A.J. Malkin, Yu.G. Kuznetsov, Structure 3 (1996) 759.
[4] F. Rosenberger, P.G. Vekilov, M. Muschol, B.R. Thomas, J. Crystal Growth 168 (1996) 1.
[5] S.D. Durbin, G. Feher, Ann. Rev. Phys. Chem. 44 (1996) 171.
[6] N.E. Chayen, T.J. Boggon, A. Cassetta, A. Deacon, T. Gleichmann, J. Habash, S.J. Harrop, J.R. Helliwell, Y.P. Nieh, M.R. Peterson, J. Raftery, E.H. Snell, A. Hadener, A.C. Niemann, D.P. Siddons, V. Stojanoff, A.W. Thompson, T. Ursby, M. Wulff, Quart. Rev. Biophys. 29 (1996) 227.
[7] A.A. Chernov, Phys. Rep. 288 (1997) 61.
[8] I. Dobrianov, K.D. Finkelstein, S.G. Lemay, R.E. Thorne, Acta Crystallogr. D 54 (1998) 922.
[9] C. Caylor, I. Dobrianov, S.G. Lemay, K.D. Finkelstein, R.E. Thorne, in preparation.
[10] I. Dobrianov, S.G. Lemay, C. Caylor, K.D. Finkelstein, R.E. Thorne, in preparation.
[11] T.L. Blundell, L.N. Johnson, Protein Crystallography, Academic Press, New York, 1976.
[12] M.A. Krivoglaz, X-ray and Neutron Diffraction in Nonideal Crystals, Springer, Berlin, 1996.
[13] A.A. Koz'ma, A.V. Arinkin, I.F. Mikhay'lov, M.Ya. Fuks, Fiz. Metal. Metalloved. 36 (1973) 596 (English transl.: Phys. Metals Metallogr. 38 (1973) 132.
[14] T.H. Metzger, J. Peisl, R. Kaufmann, J. Phys. F 13 (1983) 1103.
[15] S.D. Durbin, G. Feher, Ann. Rev. Phys. Chem. 44 (1996) 171.
[16] P.G. Vekilov, M. Ataka, T. Katsura, Acta Crystallogr. D51 (1995) 207.
[17] S.D. Durbin, G. Feher, J. Mol. Biol. 212 (1990) 763.
[18] S.D. Durbin, W.E. Carlson, J. Crystal Growth 122 (1992) 71.
[19] B.K. Tanner, X-ray Diffraction Topography, Pergamon, Oxford, 1976.
[20] R. Fourme, A. Ducruix, M. Ries-Kautt, B. Capelle, J. Synch. Rad. 2 (1995) 136.
[21] A. Shaikevitch, Z. Kam, Acta Crystallogr. A37 (1981) 871.
[22] J.R. Helliwell, J. Crystal Growth 90 (1988) 259.
[23] F. Otalora, B. Capelle, A. Ducruix, J.M. Garcia-Ruiz, Proc. Spacebound 97, unpublished.
[24] A. Authier, J. Crystal Growth 13/14 (1972) 34.
[25] J.L. Rodeau, V. Mikol, R. Giegé, P. Lutun, J. Appl. Crystallogr. 24 (1991) 135.
[26] A.V. Elgersma, M. Ataka, T. Katsura, J. Crystal Growth 122 (1992) 31.
[27] P.G. Vekilov, L.A. Monaco, B.R. Thomas, V. Stojanoff, F. Rosenberger, Acta Crystallogr. D 52 (1996) 785.
[28] W.A. Tiller, The Science of Crystallization, Cambridge University Press, Cambridge, 1991.
[29] D.M. Salunke, B. Veerapandian, R. Kodandapani, M. Vijayan, Acta Crystallogr. B 41 (1985) 431.
[30] L.J. Wilson, F.L. Suddath, J. Crystal Growth 116 (1992) 414.
[31] B.R. Thomas, P.G. Vekilov, F. Rosenberger, Acta Crystallogr. D 52 (1996) 776.
[32] B. Lorber, M. Skouri, J.P. Munch, R. Giege, J. Crystal Growth 128 (1993) 1203.

[33] C. Abergel, M.P. Nesa, J.C. Fontecilla-Camps, J. Crystal Growth 110 (1991) 11.
[34] J. Hirschler, F. Halgand, E. Forest, J.C. Fontecilla-Camps, Protein Sci. 7 (1998) 185.
[35] B.R. Thomas, private communication.
[36] Hirschler et al. (Ref. 34) found that large incorporated densities of HEWL in TEWL crystals also had no measurable effect on crystal B factors.
[37] R. Kodandapani, C.G. Suresh, M. Vijayan, J. Biol. Chem. 27 (1990) 16.
[38] H.E. Huxley, J.C. Kendrew, Acta Crystallogr. 6 (1953) 76.
[39] W.W. Webb, J. Appl. Phys. 33 (1962) 3546.
[40] Y.G. Kuznetsov, A.J. Malkin, A. Greenwood, A.J. McPherson, Struct. Biol. 14 (1995) 184.
[41] F. Rosenberger, P.G. Vekilov, M. Muschol, B.R. Thomas, J. Crystal Growth 168 (1996) 1.
[42] J.H. Konnert, P. D'Antonio, K.B. Ward, Acta Crystallogr. D 50 (1994) 603.
[43] A.J. Malkin, Y.G. Kuznetsov, T.A. Land, J.J. DeYoreo, A. McPherson, Nature Struct. Biol. 2 (1995) 956.
[44] C. Yip, M.D. Ward, Biophys. J. 71 (1996) 1071.
[45] A. McPherson, A.J. Malkin, Y.G. Kuznetsov, Structure 3 (1996) 759.
[46] V. Stojanoff, D.P. Siddons, Acta Crystallogr. A 52 (1996) 498.
[47] K. Izumi, S. Sawamura, M. Ataka, J. Crystal Growth 168 (1996) 106.
[48] V. Stojanoff, D.P. Siddons, L.A. Monaco, P. Vekilov, F. Rosenberger, Acta Crystallogr. D 53 (1997) 588.
[49] E.H. Snell, S. Weisgerber, J.R. Helliwell, E. Weckert, K. Holzer, K. Schroer, Acta Crystallogr. D 51 (1995) 1099.
[50] E.H. Snell, Proc. Spacebound 97, unpublished.
[51] L.A. Monaco, F. Rosenberger, J. Crystal Growth 129 (1993) 465.
[52] P.G. Vekilov, J.I.D. Alexander, F. Rosenberger, Phys. Rev. E 54 (1996) 6650.
[53] A.A. Chernov, H. Komatsu, in: J.P. van der Eerden, O.S.L. Bruinsma (Eds.), Science and Technology of Crystal Growth, Kluwer, Dordrecht, 1995.
[54] F.L. Ewing, E.L. Forsythe, M. van der Woerd, M.L. Pusey, J. Crystal Growth 160 (1996) 389.
[55] M. Skouri, B. Lorber, R. Giege, J.P. Munch, J.S. Candau, J. Crystal Growth 152 (1995) 209.
[56] K. Provost, M.C. Robert, J. Crystal Growth 156 (1995) 112.
[57] E. Forsythe, F. Ewing, M.L. Pusey, Acta Crystallogr. D 50 (1994) 614.
[58] E. Forsythe, M.L. Pusey, J. Crystal Growth 139 (1994) 89.
[59] P.G. Vekilov, L.A. Monaco, F. Rosenberger, J. Crystal Growth 156 (1995) 267.
[60] J. Hirschler, J.C. Fontecilla-Camps, Acta Crystallogr. D 52 (1996) 806.
[61] P.G. Vekilov, F. Rosenberger, J. Crystal Growth 158 (1996) 540.
[62] S. Vijayan, M. Vijayan, Acta Crystallogr. D 51 (1995) 390.